THE JOURNAL OF BIOLOGICAL CHEMISTRY VOL. 286, NO. 19, pp. 16879–16890, May 13, 2011

AMP-activated Protein Kinase (AMPK) Activation and Glycogen Synthase Kinase-3β (GSK-3β) Inhibition Induce Ca^{2+}-independent Deposition of Tight Junction Components at the Plasma Membrane*[S]◆

Received for publication, September 20, 2010, and in revised form, February 21, 2011 Published, JBC Papers in Press, March 7, 2011, DOI 10.1074/jbc.M110.186932

Li Zhang[‡], Francois Jouret[§1], Jesse Rinehart[¶], Jeff Sfakianos[‡‖], Ira Mellman[‡‖], Richard P. Lifton[¶], Lawrence H. Young[§], and Michael J. Caplan[‡§2]**

*From the Departments of [‡]Cell Biology, [§]Cellular and Molecular Physiology, and [¶]Genetics and the **Section of Cardiovascular Medicine, Department of Internal Medicine, Yale University School of Medicine, New Haven, Connecticut 06520 and [‖]Genentech Inc., South San Francisco, California 94080*

Extracellular Ca^{2+} is essential for the development of stable epithelial tight junctions. We find that in the absence of extracellular Ca^{2+}, AMP-activated protein kinase (AMPK) activation and glycogen synthase kinase (GSK)-3β inhibition independently induce the localization of epithelial tight junction components to the plasma membrane. The Ca^{2+}-independent deposition of junctional proteins induced by AMPK activation and GSK-3β inhibition is independent of E-cadherin. Furthermore, the nectin-afadin system is required for the deposition of tight junction components induced by AMPK activation, but it is not required for that induced by GSK-3β inhibition. Phosphorylation studies demonstrate that afadin is a substrate for AMPK. These data demonstrate that two kinases involved in regulating cell growth and metabolism act through distinct pathways to influence the deposition of the components of epithelial tight junctions.

Polarized epithelial cells possess highly specialized intercellular junctions, including adherens junctions and tight junctions. These cell junctions regulate the paracellular diffusion of small molecules and restrain the movement of proteins between the apical and the basolateral membrane compartments (1). A number of studies have demonstrated that extracellular Ca^{2+} is essential for both the development of new junctions (2–4) and the stabilization of mature junctions (5–10).

The cell adhesion molecule E-cadherin (11) enriched at adherens junctions (12) plays a critical role in epithelial cell adhesion and junction assembly (11, 13–17). The dependence of junction assembly on Ca^{2+} is likely attributable to the capacity of Ca^{2+} to stabilize E-cadherin in its adhesive state (18). Antibodies blocking the adhesion of E-cadherin also inhibit the formation of cell junctions (11, 19). Depletion of E-cadherin expression disrupts the establishment but not the maintenance of cell junctions (20). The cytoplasmic tail of E-cadherin contains a binding site for β-catenin (21), which subsequently binds α-catenin (22, 23) and then the actin cytoskeleton (24, 25).

Nectins belong to another family of cell adhesion molecules that consists of four members (26). The intercellular interactions of nectin molecules are Ca^{2+}-independent. The C termini of nectins bind the PDZ domain of afadin (27), which then binds F-actin (28). Together, the nectins and afadin constitute another system that organizes adherens junctions cooperatively with the cadherin-catenin system in epithelial cells. The nectin-afadin system can also independently support the formation of weak cell-cell junctions when cadherin-based cell junctions are absent (29). A recent study further demonstrated that nectin junctions appear during the earliest stages of epithelial cell morphogenesis and that expression of a dominant negative form of nectin causes failure of cell polarization and disruption of tight junction assembly (30).

Tight junction membrane proteins can be recruited to the cadherin- or nectin-based adhesion sites via the interactions between a tight junction scaffolding protein, zonula occludens (ZO)[3]-1, and either α-catenin (31) or afadin (32), respectively. The association between tight junction components and adherens junctions mediates the deposition of tight junction proteins to the cell surface in the early steps in tight junction assembly (33).

Our previous study using Mardin-Darby canine kidney (MDCK) epithelial cells revealed that AMPK plays a role in the regulation of epithelial tight junction assembly (34). AMPK is a serine-threonine kinase involved in the regulation of cell metabolism. Its activity increases with increasing AMP:ATP ratios (35). Elevated AMP levels render AMPK susceptible to activating phosphorylation by upstream kinases such as LKB1 (36–38).

Activation of LKB1 induces a series of epithelial cell polarization events, including the deposition of junctional proteins to a belt surrounding an apical like region. These events appear

* This work was supported, in whole or in part, by National Institutes of Health Grants DK17433 and 072614.
◆ This article was selected as a Paper of the Week.
[S] The on-line version of this article (available at http://www.jbc.org) contains supplemental Figs. S1–S6 and Table S1.
[1] Fellow of the Belgian American Educational Foundation.
[2] To whom correspondence should be addressed: Dept. of Cellular and Molecular Physiology, Yale University School of Medicine, P. O. Box 208026, New Haven, CT 06520-8026. Tel.: 203-785-7316; Fax: 203-785-4951; E-mail: michael.caplan@yale.edu.

[3] The abbreviations used are: ZO, zonula occludens; AICAR, aminoimidazole carboxamide ribonucleotide; AMPK, AMP-activated protein kinase; GSK, glycogen synthase kinase; HCM, high calcium medium; LCM, low calcium medium; MDCK, Mardin-Darby canine kidney; MRLC, myosin regulatory light chain; SILAC, stable isotope labeling by amino acids in cell culture; MEM, minimal essential medium; MRLC, myosin regulatory light chain.

to be independent of cell-cell contact and thus of intercellular interactions of adhesion (39). Interestingly, two recent studies found that localized activation of LKB1 represents an early signal for axon initiation in undifferentiated neurons (40, 41), which constitutes a critical step in neuronal polarization (42). The signal initiated by LKB1 activation induces inactivation of GSK-3β, and this event appears to be essential for axon elongation (43). GSK-3β is a serine-threonine kinase found ubiquitously in eukaryotes (44, 45), which plays important roles in many biological processes, ranging from the Wnt signaling pathway to astrocyte migration (46, 47).

In this study, we report for the first time that GSK-3β is also involved in regulating the deposition of epithelial cell junction components. We determined that AMPK activation and GSK-3β inhibition exert their effects on Ca^{2+}-independent deposition of tight junction proteins via independent pathways. We also identified afadin as a substrate for AMPK. Thus, our study demonstrates that alterations in the activities of two kinase pathways can lead independently to the deposition of tight junction components without the participation of extracellular Ca^{2+} or of the Ca^{2+}-dependent epithelial cell adhesion machinery.

EXPERIMENTAL PROCEDURES

Plasmids and Construct—pSUPER plasmids containing short hairpin interfering RNA sequences targeting canine E-cadherin, cadherin-6, and luciferase (served as a transfection control) were kindly provided by Dr. Ian Macara, University of Virginia. Detailed information about the preparation of these constructs was reported previously (20). For the shRNA construct targeting afadin, the E-cadherin RNAi sequences in the pSUPER plasmid were substituted by afadin RNAi sequences 5′-GCATGGATGCTGAGACTTA-3′ (clone 2) and 5′-GACAATCCTGCTGTCTACC-3′ (clone 5). Details of afadin shRNA construct preparation are available upon request.

Antibodies—Sheep anti-α1-AMPK was kindly provided by Dr. D. Grahame Hardie (University of Dundee). Rabbit anti-PATJ and rabbit anti-PAR3 were kindly provided by Dr. Ben Margolis (University of Michigan). Rabbit anti-pACC (Ser^{79}), anti-pan-α-AMPK, anti-pAMPK (Thr^{172}), and anti-p-β-catenin (Ser^{33}/Ser^{37}/Thr^{41}) were purchased from Cell Signaling. Rabbit anti-ZO-1, anti-occludin, and anti-claudin-1 were purchased from Zymed Laboratories Inc.. Mouse anti-E-cadherin clone 36 was purchased from BD Biosciences. Rhodamine-conjugated goat anti-rabbit IgG was purchased from Chemicon. Alexa Fluor 488-conjugated goat anti-mouse IgG and Alexa Fluor 488-conjugated goat anti-rabbit IgG were purchased from Molecular Probes. HRP-conjugated goat anti-mouse IgG and HRP-conjugated goat anti-rabbit IgG were purchased from Jackson ImmunoResearch. Rabbit anti-human-1-afadin and HRP-conjugated donkey anti-sheep IgG were purchased from Sigma. All commercially available antibodies were used according to the manufacturers' instructions.

Cell Culture and Transfection—MDCK cells were maintained in α-MEM (Invitrogen) supplemented with 10% fetal bovine serum (Invitrogen), 2 mM L-glutamine (Invitrogen), 50 units/ml penicillin (Invitrogen), and 50 μg/ml streptomycin (Invitrogen). Cells were grown in a humidified incubator at 37 °C and 5% CO_2 atmosphere.

To transiently transfect pSUPER plasmids encoding shRNA sequences targeting E-cadherin, cadherin-6, afadin, and luciferase into MDCK cells, an Amaxa nucleofector was utilized. The detailed protocols for transfecting MDCK cells using an Amaxa device have been previously reported (48).

Establishment of AMPK Knockdown Stable Cell Lines—Sequences targeting the canine AMPK α1 subunit were subcloned into pLH1, a derivative of the pSUPER plasmid. Plasmids were transfected with pVSVG into HEK-G2 cells for lentivirus packaging. Subconfluent MDCK cells were then infected with the resultant lentivirus. Selection and maintenance of stable MDCK cell clones were performed in α-MEM containing 4 μg/ml puromycin (Sigma). Clones were screened for reduced expression levels of AMPK α1 subunit by Western blot analysis. An empty pLH1 plasmid was also packaged into lentivirus, and a pooled control MDCK cell line was established by infection with this lentivirus. The sequence chosen for targeting AMPK α1 subunit was 5′-GCAGAAGTTTGTAGGGCAATT-3′.

Calcium Switch—MDCK cells were grown on plastic (for Western blot analysis) or coverslips (for immunofluorescence) in α-MEM containing 1.8 mM calcium (high calcium medium, HCM) until they formed a confluent monolayer. Cells were then washed twice with minimum essential medium for suspension culture (S-MEM, Invitrogen) and incubated in S-MEM supplemented with 5% dialyzed fetal bovine serum (Invitrogen) (low calcium medium, LCM). Cells were incubated in LCM for 16 h before being switched back to HCM for the indicated times.

Immunofluorescence and Quantification of ZO-1 Staining—Cells on coverslips were washed three times with cold PBS and fixed in 100% methanol at −20 °C for 5 min. Cells were then permeabilized in 0.3% Triton X-100, 0.15% BSA (permeabilization buffer) in PBS for 15 min at room temperature and blocked in goat serum dilution buffer (GSDB, 16% goat serum (Invitrogen), 20 mM sodium phosphate, pH 7.4, 450 mM NaCl, 0.3% Triton X-100) for 30 min at room temperature. Cells were incubated in primary antibody diluted 1:200 in GSDB for 1 h at room temperature, then immersed three times in permeabilization buffer, and then incubated for 1 h in secondary antibody diluted 1:200 in GSDB. Cells were then rinsed three times in PBS before mounting in Vectashield (Vector Laboratories). Cells were visualized on a Zeiss Axiophot fluorescence microscope equipped with a Zeiss AxioCam HRm CCD camera. Contrast and brightness settings were chosen so that all pixels were in the linear range. Pictures were taken in the focal plane in which the most strands of tight junction components were visualized.

To quantify the mean ZO-1 length per cell, four fields were randomly selected from each coverslip, and the total length of ZO-1 at the cell periphery in each field was manually outlined, followed by length measurement with ImageJ software. Cell numbers were counted for each field, and the mean ZO-1 length per cell was calculated. Statistical analysis was performed using the two-tailed Student's *t* test. In each case, the data presented are representative of at least two or three independent experimental repetitions.

Western Blot—Cells were lysed on ice in kinase lysis buffer (250 mM sucrose, 20 mM Tris-HCl, pH 7.4, 50 mM NaCl, 50 mM NaF, 5 mM sodium pyrophosphate, 1 mM Na_3VO_4, 2 mM fresh DTT, 1% Triton X-100) for 30 min. Cell lysate was centrifuged at 15,000 rpm at 4 °C for 10 min. Supernatant was then collected for Western blot. Proteins were resolved with 8% SDS-PAGE using standard protocols. The protein was electrophoretically transferred to nitrocellulose membranes (Bio-Rad) and blocked with milk solution (150 mM NaCl, 20 mM Tris, 5% milk (w/v), 0.1% Tween (v/v), pH 7.5) to quench nonspecific protein binding. The blocked membranes were probed with primary and secondary antibodies diluted in the milk solution, and the bands were visualized with the enhanced chemiluminescence kit (Amersham Biosciences).

AMPK in Vitro Phosphorylation Assay—Each AMPK *in vitro* phosphorylation assay included a pre-determined amount of immunoprecipitated proteins of interest immobilized on protein A-agarose beads (no more than 20 μl of beads), 1 μCi of [γ-^{32}P]ATP (freshly purchased from PerkinElmer Life Sciences), 50 μM ATP (Sigma), 100 μM AMP (Sigma), and 50 ng of recombinant AMPK α1β1γ2 protein complex (Cell Signaling). The assay mixtures were then incubated for 15 min at 37 °C in a solution containing 5 mM MOPS, pH 7.2, 2.5 mM β-glycerophosphate, 1 mM EGTA, 0.4 mM EDTA, 5 mM $MgCl_2$, and 50 μM DTT. The reactions were terminated by incubating mixtures at 100 °C for 5 min. The proteins of interest were then eluted from the beads by incubating with SDS sample buffer at 60 °C for 5 min. The proteins were separated by SDS-PAGE, after which the gel was dried, and the radioactive signals on the gel were revealed by autoradiography.

SILAC Labeling and LC-MS/MS Analysis—MDCK cell lines were passaged at 10% confluence onto 10-cm plates in 10 ml of heavy (0.1 mg/ml L-lysine-$^{13}C_6$ and 0.025 mg/ml L-arginine-$^{13}C_6{}^{15}N_4$) or light (normal) SILAC media. Cells were grown to confluence and then replated at 10% confluence, still in heavy or light medium, with cell numbers normalized between heavy and light conditions. After treatments, heavy and light cell lysates were prepared as a 1:1 mixture according to protein concentration, and native afadin was then immunoprecipitated.

Afadin proteins purified via immunoprecipitation and SDS-PAGE were subjected to in-gel tryptic digestion. Following digestion, total afadin peptides were subjected to titanium dioxide (TiO_2) enrichment to separate phosphopeptide (enriched) and nonphosphopeptide (flow-through) fractions for LC-MS/MS analysis.

Protein identification and SILAC quantitation were batch-processed using Mascot Daemon (version 2.2.107, β) and Mascot Distiller (version 2.3.0.0) from Matrix Science. Data base searches were conducted using our in-house Mascot Server (version 2.3.0), which has the latest quantitation Toolbox update.

RESULTS

Inhibition of GSK-3β Induces Ca^{2+}-independent Deposition of Junction Components—In the MDCK epithelial model system, low concentrations of extracellular Ca^{2+} disrupt intercellular junctions (49), and the restoration of high Ca^{2+} concentrations induces the deposition of junction proteins to the plasma membrane. This manipulation is referred to as a "Ca^{2+} switch" (49). We first sought to determine whether the activity of GSK-3β influences this process.

We cultured MDCK cells to confluency in high Ca^{2+} medium (1.8 mM Ca^{2+}, HCM) and then incubated them in low Ca^{2+} medium (5 μM Ca^{2+}, LCM) for 16 h. At 30 min and 1 and 2 h after the reintroduction of HCM, cells were lysed in the presence of phosphatase inhibitors, followed by a Western blot analysis. To examine the activity of GSK-3β, we used an antibody specifically recognizing β-catenin phosphorylated on residues $Ser^{33}/Ser^{37}/Thr^{41}$. These residues were demonstrated to be phosphorylated by GSK-3β (50). Thus, the extent of their phosphorylation indirectly reflects the *in situ* level of GSK-3β activity. We found that, despite a constant level of total β-catenin, the levels of phosphorylated β-catenin were reduced in cells lysed after the addition of HCM as compared with those detected in cells maintained in LCM, suggesting decreased GSK-3β activity during Ca^{2+}-induced epithelial polarization (Fig. 1*A*). To determine whether the decreased levels of β-catenin phosphorylation were attributable instead to the activation of phosphatases during the calcium switch, we treated MDCK cells subjected to a calcium switch with okadaic acid, which inhibits a broad spectrum of phosphatases. We found that despite an overall increase in β-catenin phosphorylation, the levels of phosphorylated β-catenin were still reduced in cells during the calcium switch (supplemental Fig. S1*A*), suggesting that the activation of phosphatases did not cause the decrease in β-catenin phosphorylation. GSK-3β was reported to be inhibited by Ser^9 phosphorylation (51). We did not detect any change in Ser^9 phosphorylation during the Ca^{2+} switch using an antibody recognizing GSK-3β phosphorylated on Ser^9, suggesting that Ser^9 phosphorylation is not responsible for GSK-3β inhibition during this process (Fig. 1*A*).

To inhibit GSK-3β pharmacologically, we treated MDCK cells with the GSK-3β inhibitors (52) 10 μM SB216763 or 20 mM LiCl for 1 h and found that both treatments decreased β-catenin phosphorylation compared with the treatments with DMSO vehicle control or with 20 mM NaCl, which reproduces the osmolarity and tonicity effects of LiCl (Fig. 1*B*). These data confirm that SB216763 and LiCl effectively inhibit GSK-3β in the MDCK cell system. We then investigated the effects of GSK-3β inhibition on the deposition of tight junction proteins by examining the time course of the localization of ZO-1 during Ca^{2+} switch in the presence or absence of GSK-3β inhibitors, and we found that ZO-1 deposition is significantly accelerated in the cells incubated in the presence of SB216763 or LiCl, compared with those incubated in DMSO or in NaCl (supplemental Fig. S1, *B* and *C*), suggesting that GSK-3β inhibition accelerates the deposition of junction proteins during Ca^{2+}-induced junction assembly.

Intriguingly, we noticed that in MDCK cells pretreated with GSK-3β inhibitors, tight junction proteins were relocalized to the sites of cell-cell contact even before the reintroduction of Ca^{2+}. We found that the deposition of ZO-1 occurs in LCM in the presence of 10 μM SB216763 or 20 mM LiCl but not in the presence of DMSO or NaCl (Fig. 1, *C* and *D*). We observed fragmentary strands of ZO-1 on plasma membranes as early as

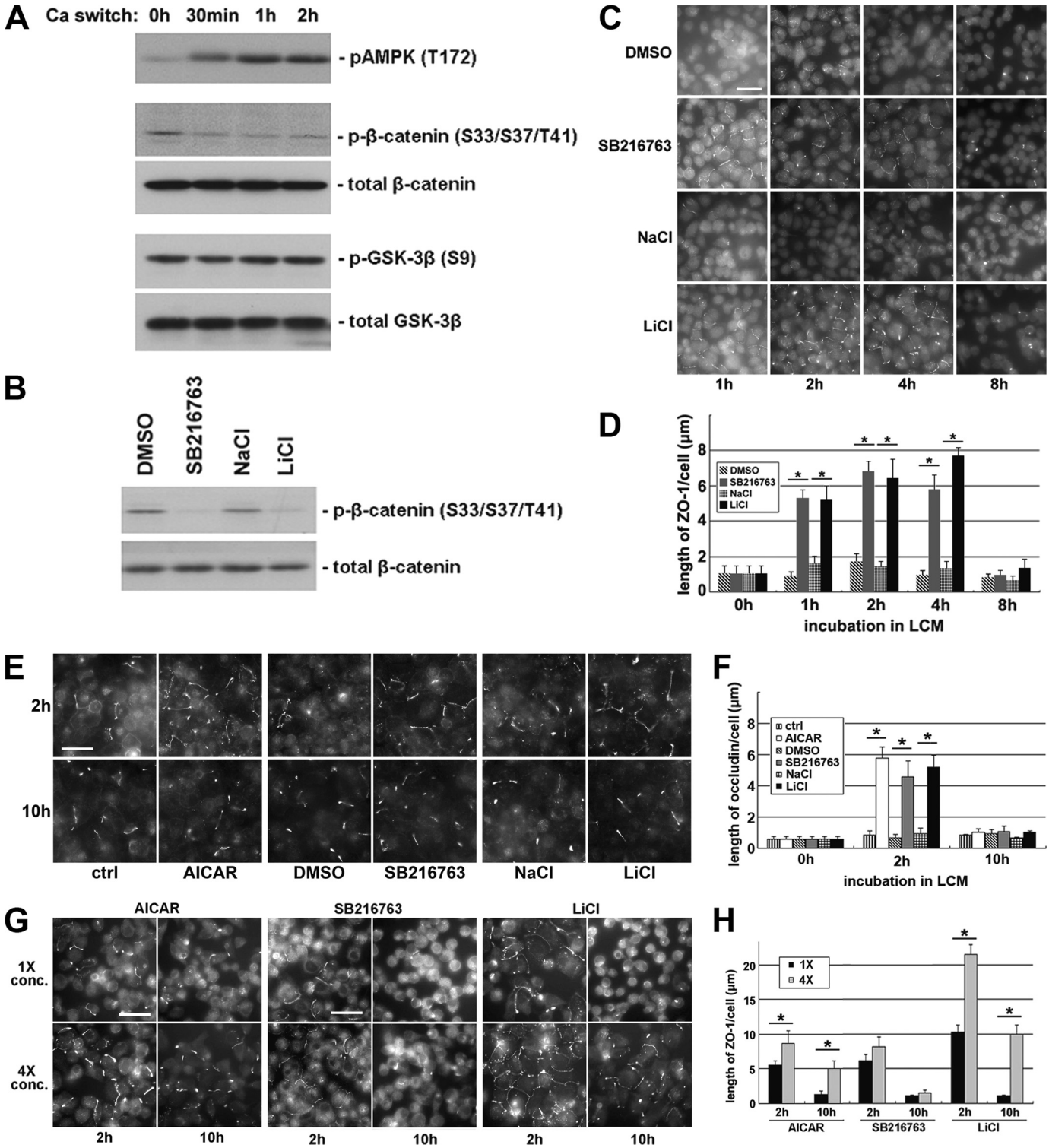

FIGURE 1. **Inhibition of GSK-3β induces Ca^{2+}-independent deposition of junction components.** *A,* confluent MDCK cells were incubated in LCM for 16 h and then switched back to HCM for the indicated times. Cell lysates were probed with the indicated antibodies in a Western blot analysis. *B,* confluent MDCK cells were treated with DMSO, 10 μM SB216763, 20 mM NaCl, or 20 mM LiCl for 2 h. Cell lysates were probed with the indicated antibodies in a Western blot analysis. *C,* confluent MDCK cells were incubated in LCM for 16 h followed by replacement of the media with fresh LCM supplemented with DMSO, 10 μM SB216763, 20 mM NaCl, or 20 mM LiCl. Cells were fixed at the indicated time points after the replacement of medium and immunostained for ZO-1. *Bar,* 30 μm. *D,* quantification of ZO-1 relocalization to cell membrane in *C*. Data are representative of three independent experiments ($n = 3$). *Error bars* represent means ± S.D. ZO-1 length per cell is within each of the four randomly picked view fields. The *asterisks* denote significant difference in the indicated pairs ($p < 0.05$) by Student's *t* test. *E,* MDCK cells were treated as described in *C*, except that they were instead immunostained for occludin. *Bar,* 30 μm. *F,* quantification of occludin relocalization to cell membrane in *E*. *Error bars* represent means ± S.D. for occludin length per cell within each of the four randomly picked view fields. The *asterisks* denote significant difference in the indicated pairs ($p < 0.05$) by Student's *t* test. *G,* confluent MDCK cells were incubated in LCM for 16 h followed by replacement of the media with fresh LCM supplemented with the indicated concentrations of different test reagents. Cells were fixed 2 and 10 h after the medium change and immunostained for ZO-1. *Bar,* 30 μm. *H,* quantification of ZO-1 relocalization to cell membrane in *G*. Data are representative of two independent experiments ($n = 2$). *Error bars* represent means ± S.D. for ZO-1 length per cell within each of the four randomly picked view fields. The *asterisks* denote significant differences in the indicated pairs ($p < 0.05$) by Student's *t* test.

1 h and throughout up to 4 h of SB216763 or LiCl treatment. However, the ZO-1 strands failed to become more consolidated and morphologically organized with further SB216763 or LiCl incubation. Instead, most of the ZO-1 strands disappeared at 8 h of continued treatment. These results appear to contradict the widely accepted notion that extracellular Ca^{2+} is required to initiate the deposition of junction components (2–4). Thus, we next studied several different proteins associated with the tight junction to assess the generality of this observation. We examined the distribution of occludin, a membrane protein that is essential for the integrity of tight junctions. Similar to what was observed with ZO-1, we found that, in cells treated with SB216763 or LiCl, fragmentary strands of occludin were detectable on the cell membrane, primarily at sites of apparent cell-cell contact. Most of these occludin strands disappear after prolonged incubation for 10 h (Fig. 1, *E* and *F*). In addition, following the treatment with SB216763 or LiCl in LCM, we observed fragmentary strands of PATJ and PAR-3, both of which are components of polarity complexes that are relocalized to the plasma membrane during junction assembly. These proteins were diffusely organized following DMSO or NaCl treatments (supplemental Fig. S1*D*). We also investigated whether or not these fragmentary junction components became tightly associated with the actin cytoskeleton. To begin to assess this possibility, we made use of a Triton X-100 extractability assay (53). We separated cell lysates into Triton-soluble and Triton-insoluble fractions. This latter pool is thought to include proteins that are strongly associated with the cytoskeleton. We did not detect any significant transition of the junction components ZO-1, occludin, or claudin from the Triton-soluble pool into the Triton-insoluble pool, suggesting that these proteins had not yet become tightly associated with the actin cytoskeleton in response to 2 h of GSK-3β inhibition (supplemental Fig. S1*E*). We did not detect any significant increase in the transepithelial electrical resistance in cells treated for 2 h with GSK-3β inhibitors (data not shown), presumably because the nascent junction-related structures that we observed were incomplete and did not produce tight seals.

We next sought to determine how different concentrations of GSK-3β inhibitors would affect the extent and the duration of the Ca^{2+}-independent deposition of junction components. We treated MDCK cells maintained in LCM with the original (10 μM SB216763 or 20 mM LiCl) or quadrupled (40 μM SB216763 or 80 mM LiCl) concentrations of GSK-3β inhibitors for both 2 and 10 h. After 2 h of treatment, we observed a significant increase in the number and length of ZO-1 strands on plasma membranes with the higher doses of the inhibitors. After 10 h of treatment with either of these high dose GSK-3β inhibitors, substantial numbers of ZO-1 strands were still retained on the plasma membrane, whereas most of the ZO-1 strands disappeared from plasma membrane in cells treated with the original concentrations of GSK-3β inhibitors (Fig. 1, *G* and *H*). We found similar results when we stained the cells for occludin (supplemental Fig. S1, *F* and *G*), confirming that higher concentrations of GSK-3β inhibitors enhance both the extent and the duration of the Ca^{2+}-independent deposition of junction components.

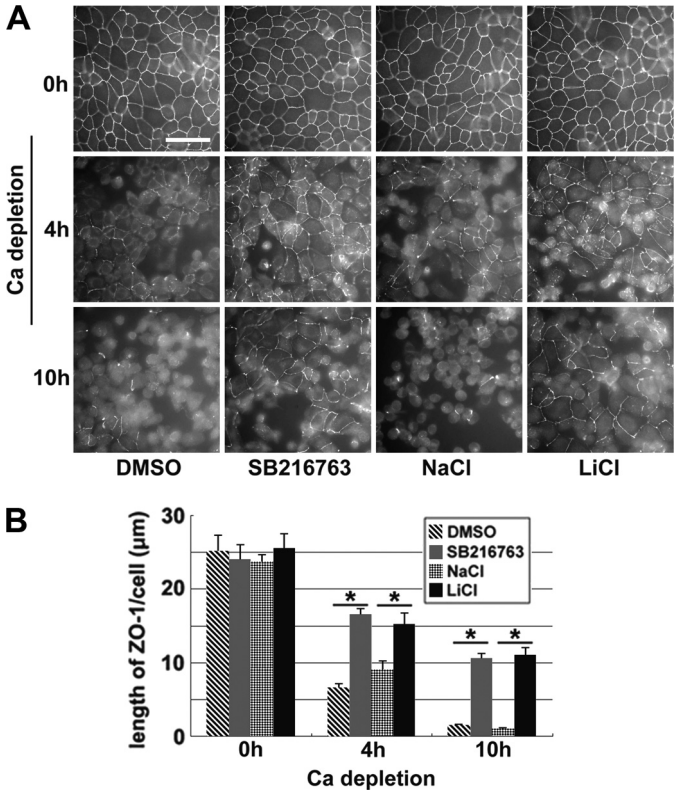

FIGURE 2. **Inhibition of GSK-3β delays the withdrawal of junction proteins from the plasma membrane upon Ca^{2+} depletion.** *A*, confluent MDCK cells were incubated in HCM with DMSO, 10 μM SB216763, 20 mM NaCl, or 20 mM LiCl for 1 h before they were switched to LCM in the presence of the aforementioned test reagents. Cells were fixed 4 and 10 h after the medium change and immunostained for ZO-1. *Bar*, 30 μm. *B*, quantification of ZO-1 on the cell membrane in *A*. Data are representative of three independent experiments ($n = 3$). *Error bars* represent means ± S.D. for ZO-1 length per cell within each of the four randomly picked view fields. The *asterisks* denote significant differences in the indicated pairs ($p < 0.05$) by Student's *t* test.

Our previous study has shown that AMPK activation induces Ca^{2+}-independent deposition of junction components to the sites of cell-cell contact (34). We found that treating cells with higher concentrations of the AMPK activator, AICAR, also enhance both the extent and the duration of the Ca^{2+}-independent deposition of junction components, as compared with that detected in cells treated with lower AICAR concentrations (Fig. 1, *E–H*).

Inhibition of GSK-3β Delays the Withdrawal of Junction Components from the Plasma Membrane upon Ca^{2+} Depletion—Depletion of Ca^{2+} from the medium causes disassembly of cell-cell junctions in polarized epithelial cells, and the junction components become diffusely distributed throughout the cytoplasm. We sought to determine whether inhibition of GSK-3β delays this process. We pretreated confluent polarized MDCK cells cultured in HCM with GSK-3β inhibitors (10 μM SB216763 or 20 mM LiCl) for 1 h and then substituted HCM with LCM, in the continued presence of these inhibitors. Cells were fixed immediately or 4 or 10 h following the medium change and were then immunostained for ZO-1. After both 4 and 10 h of Ca^{2+} depletion, we observed significantly more ZO-1 organized on the plasma membranes of cells treated with SB216763 or LiCl than on those of cells treated with DMSO or NaCl (Fig. 2). We also studied the distribution of occludin dur-

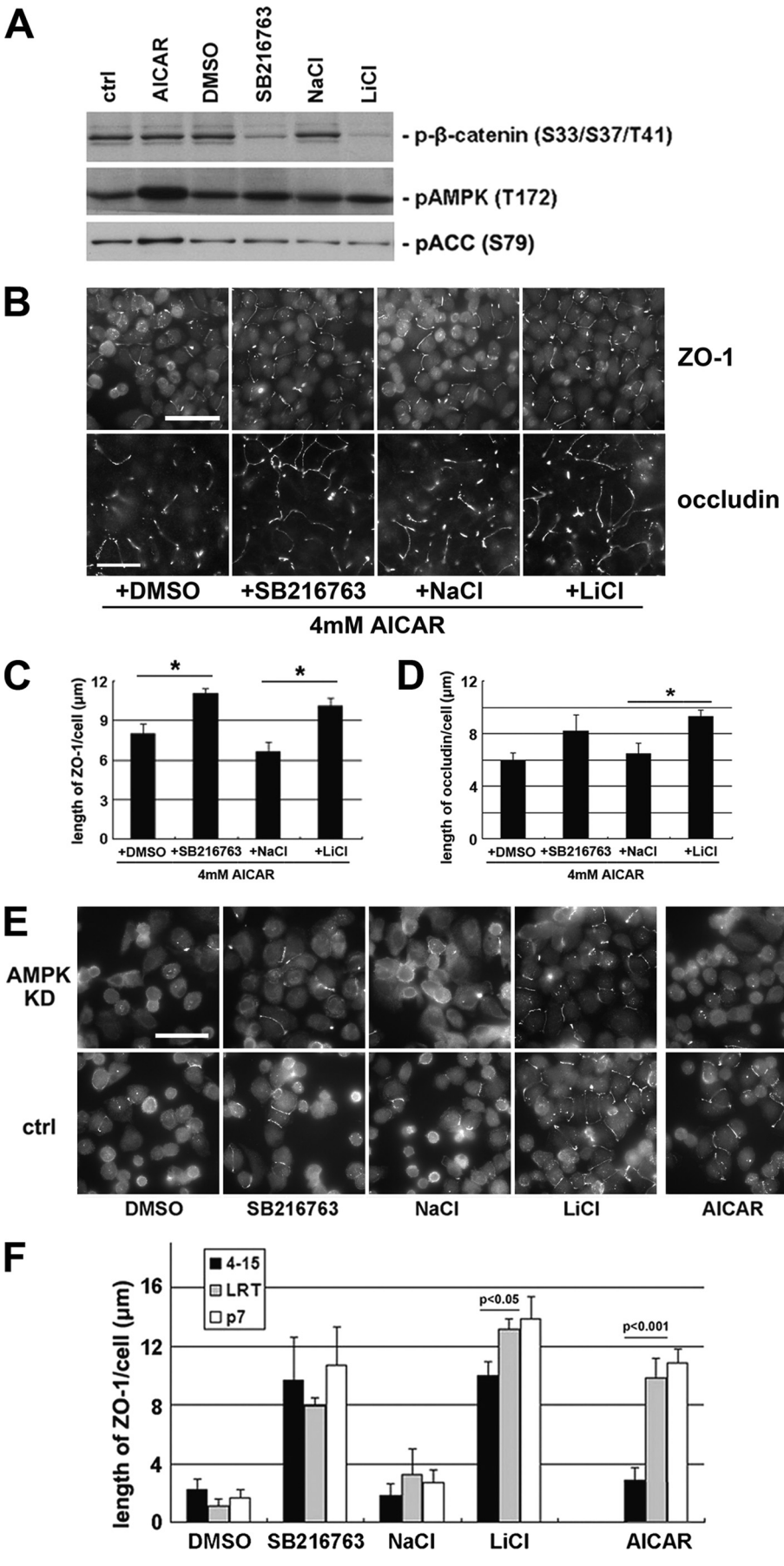

ing these treatments, and we found that significantly more occludin strands were retained on the plasma membrane after 10 h of Ca^{2+} depletion when the cells were treated with SB216763 or LiCl, compared with cells treated with DMSO or NaCl (supplemental Fig. S2). Taken together, these results demonstrate that GSK-3β inhibition delays the withdrawal of junction components from the plasma membrane when extracellular Ca^{2+} is depleted.

Activation of AMPK and Inhibition of GSK-3β Synergistically Induce Ca^{2+}-independent Deposition of Junction Components via Different Pathways—Because both AMPK activation and GSK-3β inhibition induce similar effects on the deposition of junction components, we sought to determine whether these two kinases function in the same pathway. We first examined whether AMPK activation leads to GSK-3β inhibition or vice versa. AMPK is activated by phosphorylation on residue Thr^{172}, and activated AMPK phosphorylates its substrate acetyl-CoA carboxylase (35). The phosphorylation status of AMPK and acetyl-CoA carboxylase is widely used as an indicator of AMPK activity. We treated MDCK cells with 1 mM AICAR for 2 h and found significantly higher levels of both phosphorylated AMPK and phosphorylated acetyl-CoA carboxylase, which confirms that AMPK is activated. We then examined the levels of phosphorylated β-catenin and found no significant change, suggesting that GSK-3β is not inhibited by AMPK activation (Fig. 3*A*). We next performed a reciprocal experiment by treating MDCK cells with 10 μM SB216763 or 20 mM LiCl for 1 h and then examining the levels of AMPK activity. We observed significantly lower levels of β-catenin phosphorylation but no change in the phosphorylation of either AMPK or acetyl-CoA carboxylase, suggesting that AMPK is not activated by GSK-3β inhibition (Fig. 3*A*).

We then sought to determine whether the effects of AMPK activation and GSK-3β inhibition on Ca^{2+}-independent deposition of junction components are synergistic. If GSK-3β inhibition could further promote the deposition of junction components when the effects of AMPK activation on this process are maximized, it would constitute a strong argument that the effects of AMPK activation and GSK-3β inhibition are synergistic and that they are unlikely to function in the same pathway. We found that the effects of AMPK activation are saturated at 4 mM AICAR (supplemental Fig. S3, *A* and *B*). We then combined GSK-3β inhibitors (10 μM SB216763 or 20 mM LiCl) with 4 mM AICAR in LCM and treated Ca^{2+}-depleted MDCK cells for 2 h. We were able to detect significantly more extensive ZO-1 or occludin strands on the plasma membrane with the combination of GSK-3β inhibitors and AICAR than were observed with the DMSO or NaCl in combination with AICAR (Fig. 3, *B–D*) These data indicate that GSK-3β inhibition further promotes Ca^{2+}-independent deposition of junction components under conditions in which AMPK effects are maximized, suggesting that these two molecules function synergistically via different pathways.

If AMPK and GSK-3β employ different pathways to induce Ca^{2+}-independent deposition of junction components, then elimination of AMPK activity should not influence the effects of GSK-3β inhibition. To test this hypothesis, we introduced AMPK shRNA into MDCK cells and generated stable cell lines (4-2 and 4-15) in which AMPK expression is reduced by 90% compared with those of control cell lines (P7 and LRT) (supplemental Fig. S3*C*). We found that AICAR is much less effective in inducing Ca^{2+}-independent deposition of junction components in AMPK knockdown cells, as evidenced by many fewer ZO-1 strands relocalized to the sites of cell-cell contact than those observed in control cell lines. However, when we treat AMPK knockdown cells with GSK-3β inhibitors, we detected levels of ZO-1 deposition similar to those found in control cell lines (Fig. 3, *E* and *F*). Similar results were also observed when we stained the cells for occludin (supplemental Fig. S3, *D* and *E*). We conclude that the effects of GSK-3β inhibition on the deposition of junction components are not affected by reduced AMPK activity, further suggesting that AMPK activation and GSK-3β inhibition induce Ca^{2+}-independent deposition of junction components via different pathways.

Activation of AMPK and Inhibition of GSK-3β Induce Deposition of Junction Components Independent of E-cadherin—Epithelial cells adhere to their neighbors via E-cadherin, which requires extracellular Ca^{2+} to stabilize it in its adhesive state. Blockade of adhesion inhibits the formation of the epithelial junction complex (18). Because AMPK activation and GSK-3β inhibition induce deposition of junction components independent of extracellular Ca^{2+}, we sought to determine whether this process is also independent of E-cadherin.

To test the involvement of E-cadherin, we used shRNA constructs targeting both E-cadherin and the kidney-specific cadherin-6, as well as a control construct (kindly provided by Dr. Ian Macara, University of Virginia). The efficacy of these constructs has been previously demonstrated (20). We transiently transfected these constructs into MDCK cells, cultured the cells for 48 h in HCM, and found that more than 90% of E-cadherin was eliminated (supplemental Fig. S4*A*). These cadherin knockdown cells and control cells were cultured in LCM for 16 h before being treated with 1 mM AICAR, 10 μM SB216763, or 20 mM LiCl. We found no significant difference in the amount of ZO-1 or occludin that was relocalized to plasma membrane in cadherin knockdown cells *versus* control cells, suggesting that

FIGURE 3. **AMPK activation and GSK-3β inhibition synergistically induce Ca^{2+}-independent deposition of junction components via different pathways.** *A,* MDCK cells were treated with 1 mM AICAR, DMSO, 10 μM SB216763, 20 mM NaCl, or 20 mM LiCl for 2 h. Cell lysates were probed with the indicated antibodies in a Western blot analysis. *ctrl*, control. *B,* confluent MDCK cells were incubated in LCM for 16 h followed by the replacement of the media with fresh LCM supplemented with the combination of 4 mM AICAR and DMSO, SB216763, NaCl, or LiCl. Cells were fixed 2 h after the medium change and immunostained for ZO-1 and occludin. *Bar,* 30 μm. *C* and *D,* quantification of ZO-1 and occludin relocalization, respectively, to cell membrane in *B*. Data are representatives of two independent experiments ($n = 2$) for each protein. *Error bars* represent means ± S.D. for strand length per cell within each of the four randomly picked fields of view. The *asterisks* denote significant differences in the indicated pairs ($p < 0.05$) by Student's *t* test. *E,* confluent AMPK knockdown stable MDCK cells and confluent control cells were incubated in LCM for 16 h followed by the replacement of the media with fresh LCM supplemented with DMSO, SB216763, NaCl, LiCl, or AICAR. Cells were fixed 2 h after the medium change and immunostained for ZO-1. *Bar,* 30 μm. *F,* quantification of ZO-1 relocalization to cell membrane in *E*. Data are representative of three independent experiments ($n = 3$). *Error bars* represent means ± S.D. for ZO-1 length per cell within each of the four randomly picked view fields. *p* values from Student's *t* test are noted in the figure.

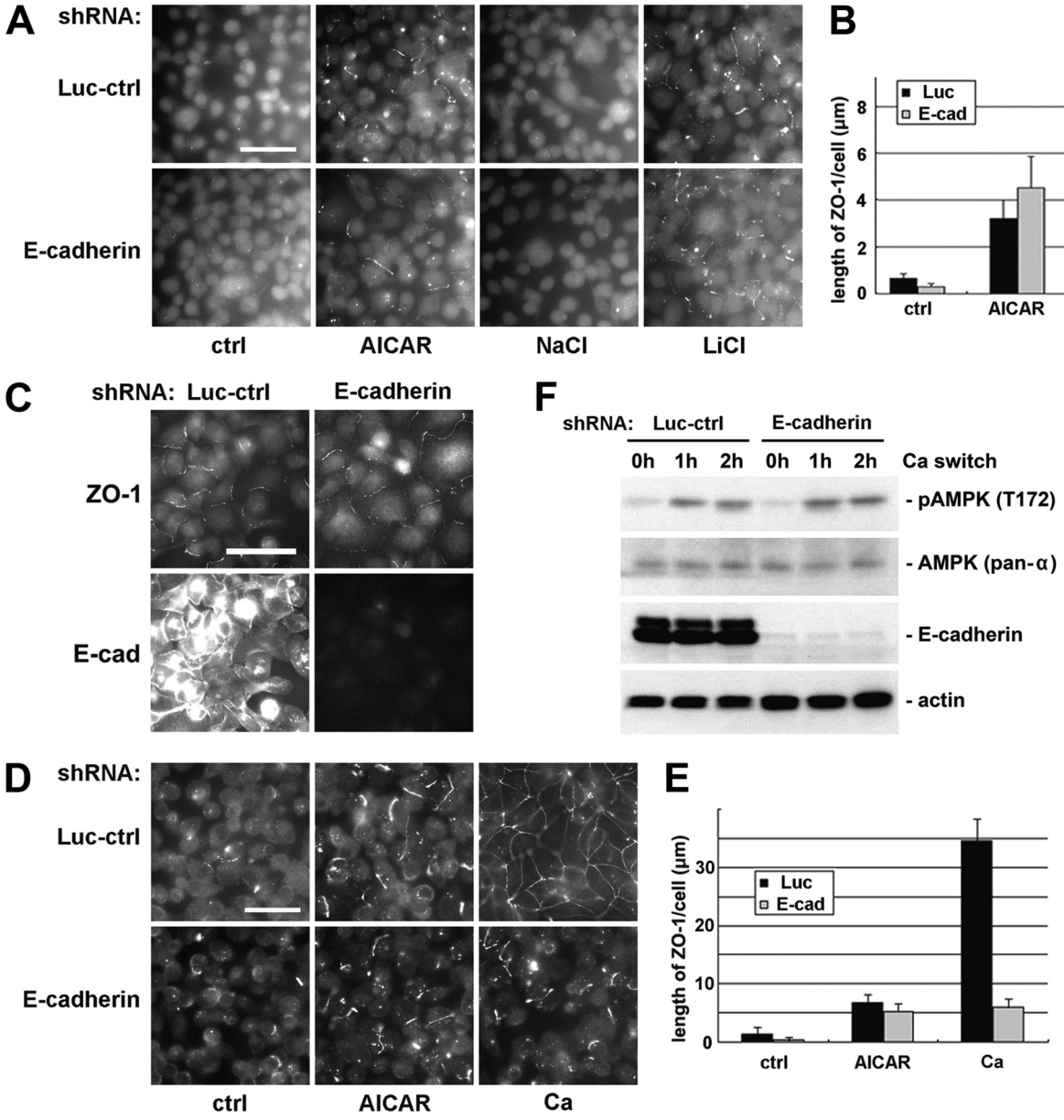

FIGURE 4. **Activation of AMPK and inhibition of GSK-3β induce deposition of junction components independent of E-cadherin.** *A,* MDCK cells transfected with E-cadherin or control shRNAs were incubated in LCM for 16 h followed by replacement of the media with fresh LCM supplemented with 1 mM AICAR, 20 mM NaCl, or 20 mM LiCl. Cells were fixed 2 h after the medium change and immunostained for ZO-1. *Bar,* 30 μm. *Luc-ctrl,* luciferase control. *B,* quantification of ZO-1 relocalization to cell membrane in *A*. Data are representative of three independent experiments ($n = 3$). *Error bars* represent means ± S.D. for ZO-1 length per cell within each of the four randomly picked view fields. *C,* MDCK cells transfected with E-cadherin or control shRNAs were incubated in LCM for 16 h followed by replacement of the media with fresh LCM supplemented with 20 mM LiCl. Cells were fixed 2 h after the medium change and immunostained for ZO-1 and E-cadherin. *Bar,* 30 μm. *D,* MDCK cells transfected with E-cadherin or control shRNAs were incubated in LCM for 16 h. Medium was replaced by fresh LCM supplemented with AICAR or HCM. Cells were fixed 2 h after the medium change and immunostained for ZO-1. *Bar,* 30 μm. *E,* quantification of ZO-1 relocalization to cell membrane in *D*. Data are representative of two independent experiments ($n = 2$). *Error bars* represent means ± S.D. for ZO-1 length per cell within each of the four randomly picked view fields. *F,* MDCK cells transfected with E-cadherin or control shRNAs were incubated in LCM for 16 h and then switched back to HCM for the indicated times. Cell lysates were probed with the indicated antibodies in a Western blot analysis.

AMPK activation and GSK-3β inhibition induce the deposition of junction components independent of E-cadherin involvement (Fig. 4, *A* and *B*, and supplemental Fig. S4, *B* and *C*). By doubly staining cell samples with antibodies directed against E-cadherin and ZO-1, we also noticed that ZO-1 was relocalized to the plasma membrane even in cells where E-cadherin expression was barely detectable (Fig. 4*C*).

We have demonstrated in a previous report that AMPK is activated during extracellular Ca^{2+}-induced junction assembly (34). Because E-cadherin is not required in Ca^{2+}-independent deposition of junction components induced by AMPK activation, we sought to determine whether extracellular Ca^{2+} could induce the deposition of junction components in cells where E-cadherin is missing. We transfected MDCK cells with shRNA constructs targeting cadherins and then subjected these cells to a Ca^{2+} switch. We found that the introduction of extracellular Ca^{2+} induced a modest but significant relocalization of junction components to the sites of cell-cell contact in cadherin knockdown cells. We compared the level of the deposition of junction components induced by extracellular Ca^{2+} with that

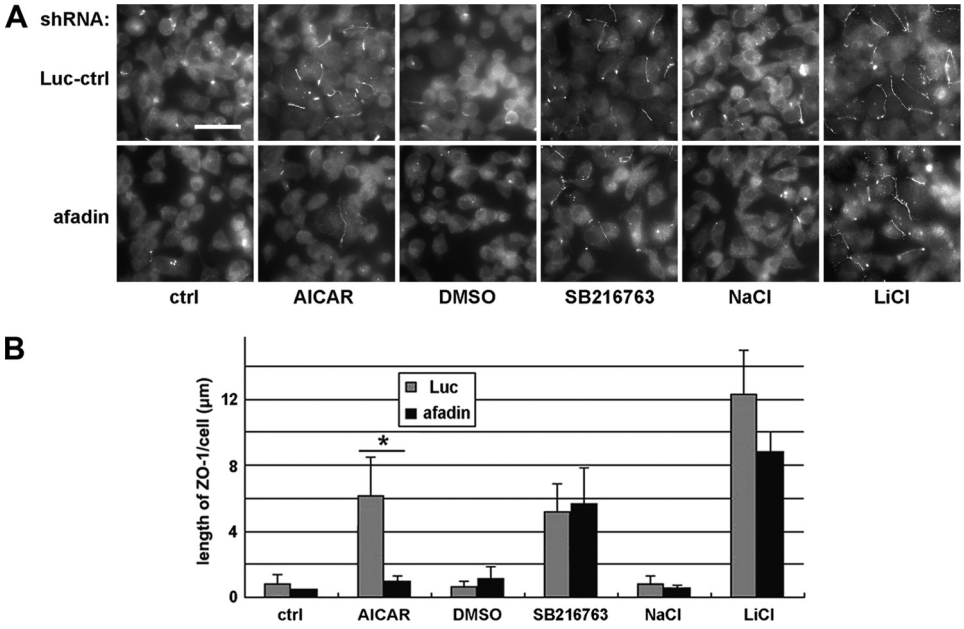

FIGURE 5. **Afadin is required to induce the deposition of junction components via AMPK activation but not via GSK-3β inhibition.** *A,* MDCK cells transfected with afadin or control shRNAs were incubated in LCM for 16 h followed by replacement of the media with fresh LCM supplemented with 1 mM AICAR, DMSO, 10 μM SB216763, 20 mM NaCl, or 20 mM LiCl. *Luc-ctrl,* luciferase control. Cells were fixed 2 h after the medium change and immunostained for ZO-1. *Bar,* 30 μm. *B,* quantification of ZO-1 relocalization to cell membrane in *A*. Data are representative of three independent experiments ($n = 3$). *Error bars* represent means ± S.D. for ZO-1 length per cell within each of the four randomly picked view fields. The *asterisk* denotes significant differences in the indicated pairs ($p < 0.05$) by Student's *t* test.

induced by the AICAR treatment in the absence of extracellular Ca^{2+}. We found that in cells where E-cadherin is depleted, these two regimens induced comparable levels of deposition of junction components (Fig. 4, *D* and *E*). It is interesting to note in this context that the Ca^{2+} switch led to AMPK activation in the E-cadherin knockdown cells, as revealed by Western blotting for phosphorylated AMPK (Fig. 4*F*). Taken together, these data are consistent with the interpretation that the E-cadherin-independent deposition of junction components stimulated by Ca^{2+} switch could be attributable to Ca^{2+} switch-induced activation of AMPK.

Afadin Is Required for AMPK Activation, but Not GSK-3β Inhibition, to Induce the Deposition of Junction Components—The nectin-afadin protein complex mediates cell adhesion independent of the cadherin-catenin mechanism. The intercellular interaction between nectin molecules does not require extracellular Ca^{2+}. Because the deposition of junction components induced by either AMPK activation or GSK-3β inhibition is independent of extracellular Ca^{2+}, we sought to investigate whether these processes are mediated by the nectin-afadin system.

To assess the involvement of the nectin-afadin system, we examined the Ca^{2+}-independent deposition of junction components in cells lacking a functional nectin-afadin complex. Nectins are a family of membrane proteins consisting of multiple members, with each member existing in a variety of splice isoforms (26). The diversity of nectins makes it difficult to efficiently eliminate their expression by the RNAi technique. Each nectin isoform, however, is linked to the actin cytoskeleton via their interaction with afadin. Therefore, knocking down afadin functionally decreases the availability of the nectin-afadin system to mediate cell-cell adhesion. We used shRNA constructs targeting afadin and the aforementioned control construct. We transiently transfected these constructs into MDCK cells, cultured these cells for 48 h in HCM, and found that about 80% of afadin was eliminated (supplemental Fig. S5*A*). These afadin knockdown cells and control cells were cultured in LCM for 16 h before they were treated with 1 mM AICAR, 10 μM SB216763, or 20 mM LiCl. We found that in afadin knockdown cells, there was no significant Ca^{2+}-independent ZO-1 or occludin relocalization induced by AICAR treatment. In control cells, however, AICAR treatment induced significantly more relocalization of ZO-1 and occludin to the plasma membrane than did the vehicle control (Fig. 5 and supplemental Fig. S5, *B* and *C*). This finding suggests that the Ca^{2+}-independent deposition of junction components induced by AMPK activation requires the nectin-afadin system. To our surprise, however, in afadin knockdown cells, both SB216763 and LiCl treatments were still able to relocalize significantly more ZO-1 and occludin to the sites of cell-cell contact compared with their respective DMSO and NaCl controls. There was no significant difference in the quantity of ZO-1 or occludin relocalized in response to GSK-3β inhibition in afadin knockdown cells *versus* control cells (Fig. 5 and supplemental Fig. S5, *B* and *C*), suggesting that GSK-3β inhibition induces deposition of junction components independent of the nectin-afadin system. This observation further supports the conclusion that AMPK activation and GSK-3β inhibition induce Ca^{2+}-independent deposition of junction components via different pathways.

Afadin Is an AMPK Substrate—Recent studies in *Drosophila* (54, 55) provide interesting clues as to how AMPK is associated with the polarization events in epithelial cells. (MRLC) was demonstrated to be phosphorylated by AMPK both in *Drosophila* and in human cells. In *Drosophila* lacking AMPK expres-

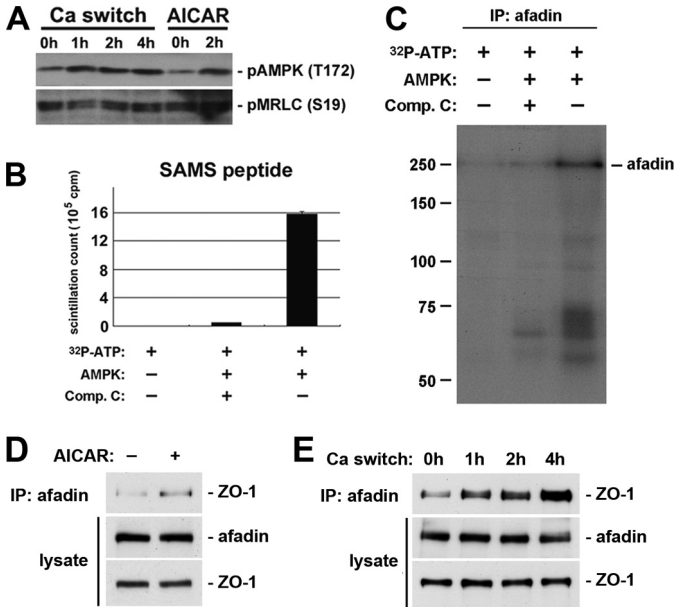

FIGURE 6. **Afadin is an AMPK substrate.** *A,* confluent MDCK cells were incubated in LCM for 16 h and then switched back to HCM for the indicated times. In addition, a separate set of MDCK cells maintained in LCM was treated with 1 mM AICAR for 2 h. Cells lysates were probed with the indicated antibodies in a Western blot analysis. *B,* AMPK was incubated with SAMS peptide along with [γ-^{32}P]ATP in the presence or absence of compound C (*Comp. C*). SAMS peptide incubated in the indicated conditions was subjected to scintillation counting. *C,* afadin in MDCK cell lysates was immunoprecipitated (*IP*), and AMPK was then added to the immunoprecipitate along with [γ-^{32}P]ATP in the presence or absence of compound C. After incubation, proteins were separated by SDS-PAGE, and the radioactive signal was detected by autoradiography. *D* and *E,* confluent MDCK cells were incubated in LCM for 16 h then switched back to HCM for the indicated times (*D*) or exposed to 1 mM AICAR for 2 h (*E*). Cell lysates were immunoprecipitated using an anti-afadin antibody. Equal amounts of immunoprecipitates were then separated on SDS-PAGE and probed for ZO-1. Total cell lysates were simultaneously subjected to immunoblotting using the anti-afadin and anti-ZO-1 antibodies.

sion, phosphorylation of Sqh (the *Drosophila* homolog of MRLC) was reduced. Transgenic expression of an activated phosphomimetic version of Sqh could rescue many aspects of the epithelial polarity defects found in *Ampkα* mutants, suggesting that AMPK regulates epithelial cell polarization primarily through its phosphorylation of MRLC. We therefore examined MRLC phosphorylation with an antibody recognizing phosphorylated human MRLC in Ca^{2+}-depleted MDCK cells treated with AICAR. We did not observe any change in MRLC phosphorylation in response to the treatment, suggesting that MRLC is not likely to be a downstream target for AMPK in inducing Ca^{2+}-independent deposition of junction components. We also examined MRLC phosphorylation in MDCK cells subjected to a Ca^{2+} switch. Although AMPK is activated in this process, we were not able to detect any concomitant change in the levels of MRLC phosphorylation (Fig. 6*A*).

The observation that the knockdown of afadin inhibits the deposition of junction components induced by AMPK activation suggests that AMPK influences afadin function, possibly by direct phosphorylation. To examine whether or not afadin is an AMPK substrate, we used an *in vitro* phosphorylation assay. We immunoprecipitated endogenous afadin from MDCK cell lysates, and the immunoprecipitated proteins were then mixed with recombinant AMPK protein and radioactively labeled [γ-^{32}P]ATP, in the presence or absence of an AMPK inhibitor compound C. After the kinase reactions were terminated, the proteins eluted from the beads were separated by SDS-PAGE. The phosphorylation profile was revealed by autoradiography. We also used an AMPK substrate, SAMS peptide, as a positive control. We found that recombinant AMPK protein was able to incorporate radioactive phosphate groups into the SAMS peptide, and this incorporation was dramatically reduced by compound C (Fig. 6*B*). The autoradiography profile of the *in vitro* phosphorylation assay revealed a band corresponding to the molecular weight of afadin in samples from the reaction in which compound C was not included, indicating that afadin was phosphorylated. In samples in which compound C was included in the reaction, the intensity of the afadin band was significantly reduced to a level comparable with that found in samples from the reactions missing the AMPK recombinant protein. These data demonstrate that AMPK activity catalyzes the incorporation of radioactive phosphate groups into afadin (Fig. 6*C*) and confirm that afadin is an AMPK substrate *in vitro*. We also performed phosphoproteomic studies on afadin immunoprecipitates prepared from intact MDCK cells to survey changes in the phosphorylation status of endogenously expressed afadin. We were able to identify afadin phosphopeptides that bear the consensus sequence for AMPK recognition and phosphorylation (supplemental Table S1). We also found that the phosphorylation on at least one of these peptides was substantially increased in cells treated with the AMPK activator AICAR. These data therefore suggest that afadin is also an AMPK substrate *in vivo* (supplemental Fig. S6).

We next sought to investigate the functional consequences of afadin phosphorylation induced by AMPK activation. Because afadin directly interacts with ZO-1 (32), we hypothesized that AMPK activation induced by either AICAR treatment or a calcium switch would increase the extent of the interaction between afadin and ZO-1, thereby facilitating the assembly of tight junctions. We immunoprecipitated afadin from cells treated with AICAR, as well as from cells lysed at different time points following a calcium switch, and then blotted the resulting immunoprecipitates to detect ZO-1 that co-precipitated with afadin. We found that in cells treated with AICAR, more ZO-1 co-precipitated with afadin compared with that detected in control cells (Fig. 6*D*). We also detected increased amounts of ZO-1 interacting with afadin in cells when the culture conditions were switched from LCM to HCM (Fig. 6*E*). These results suggested that AMPK activation might facilitate tight junction assembly by phosphorylating afadin and inducing or stabilizing its association with tight junction components such as ZO-1.

DISCUSSION

We have demonstrated that GSK-3β is involved in the regulation of an important step in epithelial cell polarization. Pharmacological inhibition of GSK-3β activity leads to the deposition of junction components to the sites of cell-cell contact in cells maintained in LCM. We found that AMPK activation and GSK-3β inhibition independently induce Ca^{2+}-independent deposition of junction components. Furthermore, the deposition of junction components in response to both treatments is

independent of E-cadherin. We also showed that the nectin-afadin cell adhesion system is required for the deposition of junction components induced by AMPK activation, but it is not required for that induced by GSK-3β inhibition. We have identified afadin as a substrate for AMPK using an *in vitro* phosphorylation assay and have shown that it is also phosphorylated *in vivo* using phosphoproteomic analysis of intact cells.

We have focused primarily on the Ca^{2+}-independent deposition of junction components in this study. To understand how the kinase activities of GSK-3β and AMPK might contribute to this process, it is worth reviewing the biological program of tight junction assembly, much of which is poorly understood. The early stages of tight junction assembly are believed to involve several critical events. First, neighboring cells must contact one another, permitting the engagement of cell adhesion molecules in a *trans*-interacting manner to form nascent cell adhesions (56). At this point, signal transduction pathways are activated that induce cytoskeleton reorganization and large scale delivery of both tight and adherens junction proteins into cell membranes (57, 58). The formation of a supporting cytoskeleton framework and the clustering of junction proteins both stabilize and strengthen the nascent cell adhesions. Subsequently, tight junction protein complexes separate from adherens junctions and move apically to form mature tight junctions (33). Under normal physiological circumstances, this process is Ca^{2+}-dependent because E-cadherin, the major arbiter of epithelial cell adhesion, requires Ca^{2+} to actively interact with its counterpart on a neighboring cell (18).

Our data suggest that, in the processes through which AMPK activation and GSK-3β inhibition induce the recruitment of tight junction components to the cell surface independent of Ca^{2+}, the prerequisite for interactions between E-cadherin molecules on the surfaces of adjacent cells can be bypassed. This may be achieved by strengthening the *trans*-interactions of other cell adhesion molecules, such as those of the nectin-afadin system, and/or by modulating cytoskeleton dynamics near the cell membrane so that nascent cell-cell contacts are more stable even without the participation of E-cadherin.

MRLC has emerged as an AMPK effector in regulating epithelial polarity in recent *Drosophila* studies (54, 55). MRLC was reported to be phosphorylated by AMPK *in vitro*, and expression of an activated phosphomimetic version of MRLC could reverse epithelial polarity defects caused by the loss of AMPK. MRLC has also been reported in many studies to be implicated in the reorganization of actin cytoskeleton. Therefore, AMPK could potentially modulate cytoskeleton dynamics by phosphorylating MRLC and thus regulating its activity. In our study, however, neither AICAR treatment nor Ca^{2+} switch induced any change in the level of MRLC phosphorylation, suggesting that MRLC is not likely an AMPK target in inducing Ca^{2+}-independent deposition of junction components, at least in the mammalian MDCK cell system.

We demonstrated that afadin can be phosphorylated by AMPK, and these findings suggest that afadin is a promising candidate to serve as the effector of AMPK in inducing junction assembly. It appears that, when AMPK is activated by AICAR, afadin plays an essential role in relocalizing tight junction components to the sites of cell-cell contact in a Ca^{2+}-independent manner. This conclusion receives support from the fact that knocking down afadin expression prevented AMPK activation from inducing Ca^{2+}-independent junction assembly. We also demonstrated that AMPK activation by either AICAR treatment or calcium switch increases the extent of the interaction between afadin and ZO-1, resulting in a connection between the nectin-afadin system and the tight junction complex. It is therefore possible that activation of the nectin-afadin system might be sufficient on its own to initiate tight junction assembly. In this context, it is interesting to note that nectin junctions are formed very early in the process of epithelial morphogenesis in the developing kidney and that nectin expression occurs prior to that of the transmembrane tight junction protein occludin. Furthermore, expression of a dominant negative nectin protein disrupts epithelial cyst formation when MDCK cells are grown in three-dimensional collagen gels (30). Taken together with our findings, these data suggest the interesting possibility that AMPK may act to initiate or reinforce nectin-afadin-mediated junction formation at an early stage of cell junction assembly, after which the formation of fully mature junctions is carried forward by Ca^{2+} and E-cadherin-dependent processes.

Although a number of recent advances link AMPK with epithelial cell polarity, the role of GSK-3β in the regulation of cytoskeleton dynamics and cell polarity has not been as extensively studied. In neurons, GSK-3β inhibition ensures the extension of axons by preventing axonal microtubules from being disrupted by the GSK-3β substrate CRMP-2. The PI3K pathway and Akt have been shown to be required for GSK-3β inhibition in this process (43). In migrating astrocytes, Cdc42 and PAR6 promote the activation of atypical PKCζ at the leading edge, which consequently phosphorylates and inhibits GSK-3β, leading to the reorganization of cytoskeleton via adenomatous polyposis coli (47, 59).

Although the upstream and downstream molecules involved in the deposition of junction components induced by GSK-3β inhibition are still under investigation, our study has provided some clues in this regard. GSK-3β is known to be inhibited when its Ser^9 residue is phosphorylated by several upstream kinases such as Akt and atypical PKCζ. We determined, however, that although the activity of GSK-3β is inhibited, the level of GSK-3β Ser^9 phosphorylation remained constant during junction assembly, suggesting that in this process GSK-3β is inhibited through a mechanism independent of Ser^9 phosphorylation and thus independent of its regulation by Akt and atypical PKCζ.

In summary, we have identified AMPK and GSK-3β as effectors in novel kinase pathways that lead to the deposition of junction components without the participation of extracellular Ca^{2+} or of the Ca^{2+}-dependent epithelial cell adhesion machinery. We also identified afadin as a substrate for AMPK in this process. Future investigation will be required to identify the downstream targets of GSK-3β, as well as to fully understand the roles that each of these pathways play in junction formation *in vivo*.

Acknowledgments—We thank Dr. D. Grahame Hardie for AMPK α1 antibody; Dr. Ian Macara for RNAi constructs; Dr. Agnes Kim for help with the AMPK activity assay; OrLando Yarborough for help with the SILAC labeling; and all members of the Caplan laboratory for insightful advice and discussions.

REFERENCES

1. Van Itallie, C. M., and Anderson, J. M. (2004) *Physiology* **19,** 331–338
2. Cereijido, M., Meza, I., and Martínez-Palomo, A. (1981) *Am. J. Physiol.* **240,** C96–C102
3. Gonzalez-Mariscal, L., Chávez de Ramírez, B., and Cereijido, M. (1985) *J. Membr. Biol.* **86,** 113–125
4. Martinez-Palomo, A., Meza, I., Beaty, G., and Cereijido, M. (1980) *J. Cell Biol.* **87,** 736–745
5. Galli, P., Brenna, A., Camilli de, P., and Meldolesi, J. (1976) *Exp. Cell Res.* **99,** 178–183
6. Hays, R. M., Singer, B., and Malamed, S. (1965) *J. Cell Biol.* **25,** (suppl.) 195–208
7. Meldolesi, J., Castiglioni, G., Parma, R., Nassivera, N., and De Camilli, P. (1978) *J. Cell Biol.* **79,** 156–172
8. Palant, C. E., Duffey, M. E., Mookerjee, B. K., Ho, S., and Bentzel, C. J. (1983) *Am. J. Physiol.* **245,** C203–C212
9. Pitelka, D. R., and Taggart, B. N. (1983) *J. Cell Biol.* **96,** 606–612
10. Sedar, A. W., and Forte, J. G. (1964) *J. Cell Biol.* **22,** 173–188
11. Gumbiner, B. (1988) *Trends Biochem. Sci.* **13,** 75–76
12. Boller, K., Vestweber, D., and Kemler, R. (1985) *J. Cell Biol.* **100,** 327–332
13. Birchmeier, C., and Birchmeier, W. (1993) *Annu. Rev. Cell Biol.* **9,** 511–540
14. Marrs, J. A., Andersson-Fisone, C., Jeong, M. C., Cohen-Gould, L., Zurzolo, C., Nabi, I. R., Rodriguez-Boulan, E., and Nelson, W. J. (1995) *J. Cell Biol.* **129,** 507–519
15. McNeill, H., Ozawa, M., Kemler, R., and Nelson, W. J. (1990) *Cell* **62,** 309–316
16. Rodriguez-Boulan, E., and Nelson, W. J. (1989) *Science* **245,** 718–725
17. Takeichi, M. (1990) *Annu. Rev. Biochem.* **59,** 237–252
18. Ringwald, M., Schuh, R., Vestweber, D., Eistetter, H., Lottspeich, F., Engel, J., Dölz, R., Jähnig, F., Epplen, J., and Mayer, S., (1987) *EMBO J.* **6,** 3647–3653
19. Gumbiner, B., and Simons, K. (1986) *J. Cell Biol.* **102,** 457–468
20. Capaldo, C. T., and Macara, I. G. (2007) *Mol. Biol. Cell* **18,** 189–200
21. Huber, A. H., and Weis, W. I. (2001) *Cell* **105,** 391–402
22. Aberle, H., Butz, S., Stappert, J., Weissig, H., Kemler, R., and Hoschuetzky, H. (1994) *J. Cell Sci.* **107,** 3655–3663
23. Pokutta, S., and Weis, W. I. (2000) *Mol. Cell* **5,** 533–543
24. Pokutta, S., Drees, F., Takai, Y., Nelson, W. J., and Weis, W. I. (2002) *J. Biol. Chem.* **277,** 18868–18874
25. Rimm, D. L., Koslov, E. R., Kebriaei, P., Cianci, C. D., and Morrow, J. S. (1995) *Proc. Natl. Acad. Sci. U.S.A.* **92,** 8813–8817
26. Takai, Y., and Nakanishi, H. (2003) *J. Cell Sci.* **116,** 17–27
27. Reymond, N., Borg, J. P., Lecocq, E., Adelaide, J., Campadelli-Fiume, G., Dubreuil, P., and Lopez, M. (2000) *Gene* **255,** 347–355
28. Mandai, K., Nakanishi, H., Satoh, A., Obaishi, H., Wada, M., Nishioka, H., Itoh, M., Mizoguchi, A., Aoki, T., Fujimoto, T., Matsuda, Y., Tsukita, S., and Takai, Y. (1997) *J. Cell Biol.* **139,** 517–528
29. Yamada, A., Fujita, N., Sato, T., Okamoto, R., Ooshio, T., Hirota, T., Morimoto, K., Irie, K., and Takai, Y. (2006) *Oncogene* **25,** 5085–5102
30. Brakeman, P. R., Liu, K. D., Shimizu, K., Takai, Y., and Mostov, K. E. (2009) *Am. J. Physiol. Renal Physiol.* **296,** F564–F574
31. Itoh, M., Nagafuchi, A., Moroi, S., and Tsukita, S. (1997) *J. Cell Biol.* **138,** 181–192
32. Yamamoto, T., Harada, N., Kano, K., Taya, S., Canaani, E., Matsuura, Y., Mizoguchi, A., Ide, C., and Kaibuchi, K. (1997) *J. Cell Biol.* **139,** 785–795
33. Rajasekaran, A. K., Hojo, M., Huima, T., and Rodriguez-Boulan, E. (1996) *J. Cell Biol.* **132,** 451–463
34. Zhang, L., Li, J., Young, L. H., and Caplan, M. J. (2006) *Proc. Natl. Acad. Sci. U.S.A.* **103,** 17272–17277
35. Hardie, D. G. (2007) *Nat. Rev. Mol. Cell Biol.* **8,** 774–785
36. Hawley, S. A., Boudeau, J., Reid, J. L., Mustard, K. J., Udd, L., Mäkelä, T. P., Alessi, D. R., and Hardie, D. G. (2003) *J. Biol.* **2,** 28
37. Hong, S. P., Leiper, F. C., Woods, A., Carling, D., and Carlson, M. (2003) *Proc. Natl. Acad. Sci. U.S.A.* **100,** 8839–8843
38. Woods, A., Johnstone, S. R., Dickerson, K., Leiper, F. C., Fryer, L. G., Neumann, D., Schlattner, U., Wallimann, T., Carlson, M., and Carling, D. (2003) *Curr. Biol.* **13,** 2004–2008
39. Baas, A. F., Kuipers, J., van der Wel, N. N., Batlle, E., Koerten, H. K., Peters, P. J., and Clevers, H. C. (2004) *Cell* **116,** 457–466
40. Barnes, A. P., Lilley, B. N., Pan, Y. A., Plummer, L. J., Powell, A. W., Raines, A. N., Sanes, J. R., and Polleux, F. (2007) *Cell* **129,** 549–563
41. Shelly, M., Cancedda, L., Heilshorn, S., Sumbre, G., and Poo, M. M. (2007) *Cell* **129,** 565–577
42. Craig, A. M., and Banker, G. (1994) *Annu. Rev. Neurosci.* **17,** 267–310
43. Jiang, H., Guo, W., Liang, X., and Rao, Y. (2005) *Cell* **120,** 123–135
44. Embi, N., Rylatt, D. B., and Cohen, P. (1980) *Eur. J. Biochem.* **107,** 519–527
45. Woodgett, J. R. (1990) *EMBO J.* **9,** 2431–2438
46. Doble, B. W., and Woodgett, J. R. (2003) *J. Cell Sci.* **116,** 1175–1186
47. Etienne-Manneville, S., and Hall, A. (2003) *Nature* **421,** 753–756
48. Chen, X., and Macara, I. G. (2006) *Methods Enzymol.* **406,** 362–374
49. Cereijido, M., Robbins, E. S., Dolan, W. J., Rotunno, C. A., and Sabatini, D. D. (1978) *J. Cell Biol.* **77,** 853–880
50. Liu, C., Li, Y., Semenov, M., Han, C., Baeg, G. H., Tan, Y., Zhang, Z., Lin, X., and He, X. (2002) *Cell* **108,** 837–847
51. Cross, D. A., Alessi, D. R., Cohen, P., Andjelkovich, M., and Hemmings, B. A. (1995) *Nature* **378,** 785–789
52. Klein, P. S., and Melton, D. A. (1996) *Proc. Natl. Acad. Sci. U.S.A.* **93,** 8455–8459
53. Tsukamoto, T., and Nigam, S. K. (1999) *Am. J. Physiol.* **276,** F737–F750
54. Lee, J. H., Koh, H., Kim, M., Kim, Y., Lee, S. Y., Karess, R. E., Lee, S. H., Shong, M., Kim, J. M., Kim, J., and Chung, J. (2007) *Nature* **447,** 1017–1020
55. Mirouse, V., Swick, L. L., Kazgan, N., St Johnston, D., and Brenman, J. E. (2007) *J. Cell Biol.* **177,** 387–392
56. Adams, C. L., Chen, Y. T., Smith, S. J., and Nelson, W. J. (1998) *J. Cell Biol.* **142,** 1105–1119
57. Vleminckx, K., and Kemler, R. (1999) *BioEssays* **21,** 211–220
58. Yonemura, S., Itoh, M., Nagafuchi, A., and Tsukita, S. (1995) *J. Cell Sci.* **108,** 127–142
59. Etienne-Manneville, S., and Hall, A. (2003) *Curr. Opin. Cell Biol.* **15,** 67–72